INTERNATIONAL JOURNAL OF PRECISION ENGINEERING AND MANUFACTURING Vol. 16, No. 7, pp. 1305-1310 JUNE 2015 / 1305
DOI: 10.1007/s12541-015-0170-6 ISSN 2234-7593 (Print) / ISSN 2005-4602 (Online)

Effect of the Surfactant on Size of Nickel Nanoparticles Generated by Liquid-Phase Plasma Method

Heon Lee[1], Minchul Chung[2], Ho-Geun Ahn[2], Sun-Jae Kim[3], Young-Kwon Park[4], and Sang-Chul Jung[1,#]

1 Department of Environmental Engineering, Sunchon National University, 255, Jungang-ro, Suncheon-si, Jeollanam-do, 540-950, South Korea
2 Department of Chemical Engineering, Sunchon National University, 255, Jungang-ro, Suncheon-si, Jeollanam-do, 540-950, South Korea
3 Faculty of Nanotechnology and Advanced Materials Engineering, Sejong University, 209, Neungdong-ro, Gwangjin-gu, Seoul, 143-747, South Korea
4 School of Environmental Engineering, University of Seoul, 163, Seoulsiripdae-ro, Dongdaemun-gu, Seoul, 130-743, South Korea
Corresponding Author / E-mail: jsc@sunchon.ac.kr, TEL: +82-61-750-3814, FAX: +82-61-750-3810

KEYWORDS: Liquid-phase plasma, Nanoparticle, Nickel, SDS, CTAB

The effect of anionic and cationic surfactants on the generation of nickel nanoparticles in a liquid-phase plasma was investigated. The size and morphology of nanoparticles generated under different conditions were observed. When no surfactant was added, more and larger particles were generated under a longer plasma treatment time and a higher electrical conductivity of the solution. When an anionic surfactant SDS was added, spherical nickel nanoparticles with various sizes were generated, with no clear evidence for the effect of SDS observed. When a cationic surfactant CTAB was added, very small nanoparticles (≤ 10 nm) could be obtained with a short reaction time. When the reaction time was too long (≥ 60 minutes), larger polygonal or wisker-shaped particles were generated.

Manuscript received: May 22, 2014 / Revised: January 14, 2015 / Accepted: March 10, 2015

1. Introduction

Synthesis and application of metal nanoparticles is the subject of intense research because of their unique physical and chemical properties. It is important to understand the properties of nanoparticles in view both of the progress in scientific knowledge and of the technological significance of enhancing the performance of existing materials.[1-6] As a kind of nanosized metallic materials, nano-nickel materials exhibit unusual electronic, magnetic, and chemical properties significantly different from the bulk materials due to their extremely small size and large specific surface area.[7-10] They have various potential applications, such as battery material, catalyst, magnetic material, nanometer coating material, and hard alloy adhesive agent.[11]

A number of techniques, such as chemical vapor deposition (CVD),[12] laser-driven aerosol,[13] hydrothermal method,[14] and microemulsion,[15] have been used for the preparation of nickel nanomaterials. But the application of the above-mentioned methods in industry is limited. One way to solve the problem is using the chemical reduction in liquid phase. During recent few years, application of plasma systems to production of nanoparticles have become of topical interest. In particular, glow discharge in liquid phase is a useful tool for synthesis of metal nanoparticles.[16,17] Liquid-phase plasma (LPP) can potentially fabricate metal nanoparticles rapidly without adding reducing agents because plasma provides a reaction field with highly excited energy states.

In this work, the LPP reduction method was applied to prepare nickel nanoparticles from the solution of nickel chloride using a bipolar pulsed electrical discharge system. The effects of the addition of a cationic surfactant cetyltrimethyl ammonium bromide (CTAB) and an anionic surfactant sodium dodecyl sulfate (SDS) on the size and morphology of the nickel particles generated from the LPP process were investigated.

2. Experimental

All the chemicals used in this work were of reagent grade and used without any further purification. Nickel chloride hexahydrate (Junsei Chemical Co., Ltd) was used to prepare 300 ml of $NiCl_2$ solutions with the $NiCl_2$ concentrations of 2.2, 3.3 and 4.5 mM. The electrical conductivities of the three solutions prepared in this way were about 500, 750 and 1,000 μs/cm, respectively. LPP process was used to fabricate Ni nanoparticles from the solutions containing Ni ions. To prevent coagulation among the Ni nanoparticles, SDS (Tokyo chemical Co., Ltd) and CTAB (Daejung Chemicals & metals Co., Ltd) were used as surfactants. The surfactant modification conditions are summarized

Table 1 Chemical concentrations and conductivity of solution used in this study

$NiCl_2$ Conc. (mM)	CTAB (g)	SDS (g)	Surfactant/$NiCl_2$ molar ratio (%)	Conductivity (μS/cm)
2.2	-	-	-	500
3.3	-	-	-	750
4.4	-	-	-	1000
3.3	0.061	-	10	750
3.3	0.121	-	20	750
3.3	0.182	-	30	750
3.3	0.243	-	40	750
3.3	0.304	-	50	750
3.3	-	0.056	10	750
3.3	-	0.112	20	750
3.3	-	0.168	30	750
3.3	-	0.224	40	750
3.3	-	0.280	50	750

in Table 1. The water used in this work was ultrapure water (Daejung Chemicals & metals Co., Ltd).

A schematic diagram of the experimental device used in this work is shown in Fig. 1. The pulsed electric discharge was generated by a needle-to-needle electrode geometry system in an annular tube type reactor (outer diameter 40 mm, height 80 mm). Tungsten electrodes (2 mm, 99.95% purity, T.T.M Korea Co.) with ceramic insulator coating were used with an interelectrode gap of 0.3 mm. The reactant solutions were thermally equilibrated in a cold water bath at 298 K and then circulated into the reactor using a roller pump. In this study, a high-frequency bipolar pulse power supply (Nano technology lnc., NTI-500W) was utilized to generate pulsed electrical plasma discharge directly in liquid phase. The reason to employ a bipolar pulse system comes from the expectation of symmetrical plasma generation and immediate cleaning of the tip of both electrodes from any possible products adjacent to either cathode or anode, and thus to ensure stable operation conditions. The applied voltage, pulse width, and frequency were 250 V, 5 μs, and 30 kHz, respectively. It was possible to generate plasma using the power supply used in this study only within the frequency range of 25~30 kHz under the conditions of discharge voltage 250 V and the pulse width 2 μs. The plasma intensity was highest when the frequency was 30 kHz. When the experiment was performed with the frequency of 25 kHz, the amount of particles produced was much smaller because the plasma generation was less vigorous, while the particle size was similar. Therefore, only the results obtained with the frequency of 30 kHz are presented in this paper. Size, morphology, and degree of dispersion of the generated nickel nanoparticles were observed using a transmission electron microscope (TEM) (FEI, Tecnai20), while size distribution and zeta potential were measured using an electrophoretic light scattering spectrophotometer (ELS-8000, Otsuka). However, it was not possible to obtain reliable results from the zeta potential measurement because nickel is a ferromagnetic substance. The particle size measured using ELS-8000 was larger than that observed by the TEM. This result seems to stem from the mechanism of particle size determination of the light scattering instrument; a cloud of separate particles located very close to one another is recognized as a single particle. Therefore, the size distribution and the zeta potential measured by ELS-8000 are not reported in this paper.

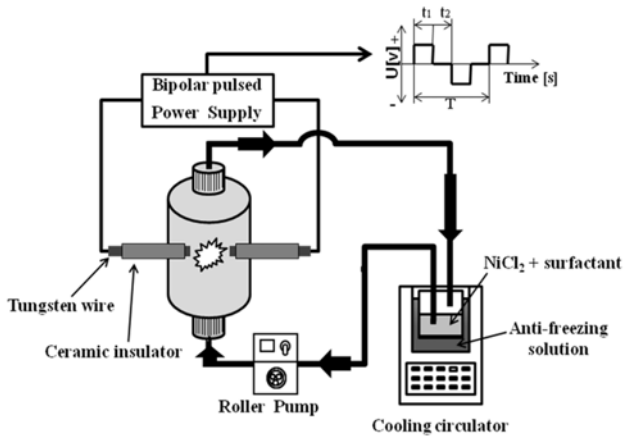

Fig. 1 Schematic of the liquid-phase plasma apparatus with high-frequency bipolar pulse power supply

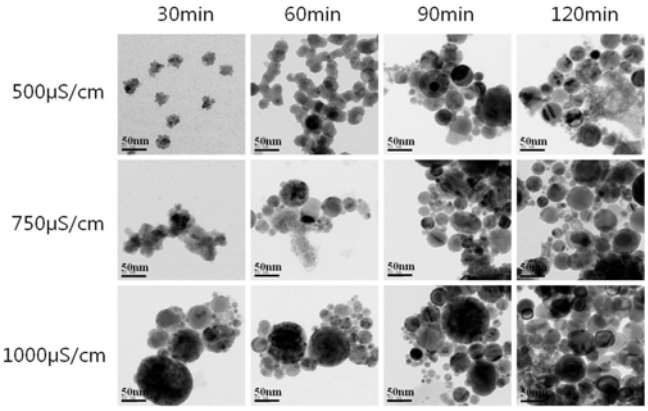

Fig. 2 TEM images of nickel nanoparticles synthesized using electrical discharge in aqueous solution without surfactant

3. Results and Discussion

3.1 Nickel nanoparticles synthesized without surfactant

Fig. 2 shows the TEM images of nickel nanoparticles obtained with different discharge times. The plasma treatment was conducted with discharge voltage of 250 V, frequency of 30 kHz, and pulse width of 5 μs. The electrical conductivities of the three solutions with the $NiCl_2$ concentrations of 2.2, 3.3, and 4.5 mM were about 500, 750, and 1,000 μS/cm, respectively. Surfactant was not used at this stage. It is shown in Fig. 2 that spherical nanoparticles with various sizes were generated by the plasma treatment. Both the particle size and the particle number were observed to increase with the length of plasma treatment time.

The effect of the electrical conductivity is also clearly shown in Fig. 2; the number and the size of generated particles increased with increasing electrical conductivity, i.e., with increasing $NiCl_2$ concentration. The size range of the produced nickel particles was measured to be 20~50 nm (30 min), 30~60 nm (60 min), 30~70 nm (90 min), and 40~60 nm (120 min) with the electrical conductivity of 500 μS; 40~60 nm (30 min), 30~70 nm (60 min), 30~80 nm (90 min), and 40~90 nm (120 min) with the electrical conductivity of 750 μS; and 50 ~90 nm (30 min), 30~100 nm (60 min), 30~110 nm (90 min), and 40~

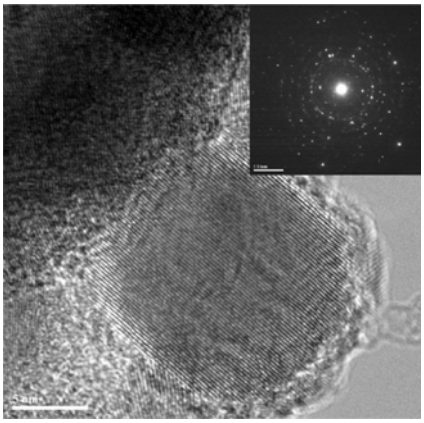

Fig. 3 High-resolution TEM image of nickel nanoparticles and corresponding ED pattern

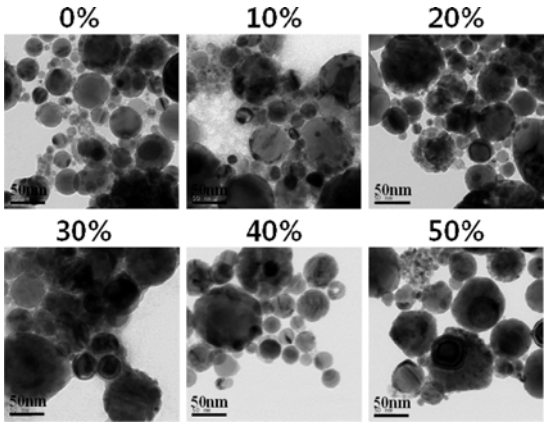

Fig. 5 TEM images of nickel nanoparticles synthesized using electrical discharge in aqueous solution with different initial SDS doses

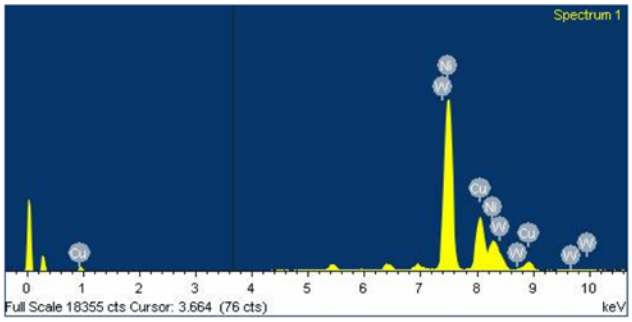

Fig. 4 EDX spectrum of nickel nanoparticles synthesized using the liquid-phase plasma method

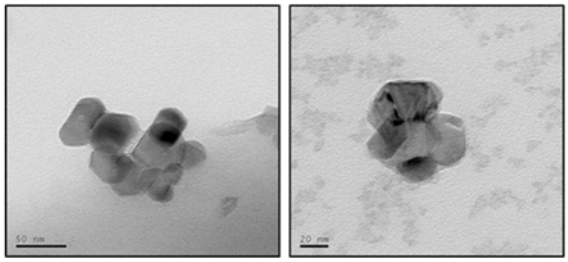

Fig. 6 TEM images of nickel pentagonal and hexagonal nanoparticles synthesized using LPP method with SDS

90 nm (120 min) with the electrical conductivity of 1,000 μS.

Fig. 3 shows a high-resolution TEM image and the ED pattern of nickel nanoparticles. Formation of crystal lattice is clearly shown in this figure. The ED pattern shows that diffraction points corresponding to the crystal direction of the lattice are observed at various directions indicating polycrystalline structure. In the meantime, the diffraction points did not comprise in complete circles, which indicates that nanoparticles are mixed with much larger particles.

An EDX spectrum (see Fig. 4) was obtained from the same nickel nanoparticle sample as that used for the TEM analysis shown in Fig. 3. Fig. 4 demonstrates the distinct presence of nickel peaks. One can also see the Cu peaks due to the presence of the Cu grid used as a support for Ni nanoparticles. Peaks for tungsten, which were used as the electrode, were also observed. The atomic %'s of these components were 73.57% (Ni), 23.23% (Cu), and 3.20 % (W).

3.2 Effect of anionic surfactant on nickel particle generation

The effects of the addition of surfactants on the particle size, the particle shape, and the dispersion of the nickel nanoparticles generated in the LPP system were investigated in this study. An anionic surfactant SDS and a cationic surfactant CTAB were used. For all the experiments described in this and the next subsections, the solution with the initial $NiCl_2$ concentration of 3.3 mM (the electrical conductivity of 750 μs/cm) was plasma-treated for 2 hours with different amounts of surfactant added. Fig. 5 shows the TEM images of the nickel nanoparticles generated by adding 0~50% SDS (the surfactant/$NiCl_2$ molar ratio %). All images obtained with different amounts of SDS addition showed similar particle size and number, indicating that the addition of an anionic surfactant SDS has negligible effect on the properties of the nickel nanoparticles generated in the LPP process. The particle size range was 20~70 nm (0%), 20~80 nm (10%), 30~80 nm (20%), 30~90 nm (30%), 20~90 nm (40%), and 30~80 nm (50%).

Fig. 6 shows the TEM images of pentagonal and hexagonal nanoparticles generated from the aqueous solution by LPP with SDS. While spherical nickel nanoparticles were mostly observed in the LPP process with SDS, pentagonal and hexagonal nanoparticles were also observed occasionally as is shown in this figure. Spherical particles are generated when the surface energies of various crystal faces do not differ from one another, which is the case for very small particles. Surface energy stems from the breakage of inter-atomic bonds of the atoms located at the surface. When a particle is small, the value of surface energy does not depend significantly on the crystal orientation. As a particle grows, however, total surface energy can vary considerably depending on the crystal orientation. Thus, crystal orientation is determined in such a way that the total surface energy can be minimized, resulting in polyhedral particle shape of large particles.

3.3 Effect of cationic surfactant on nickel particle generation

Fig. 7 shows the TEM images of the nickel nanoparticles generated by adding 0~50% CTAB (the surfactant/$NiCl_2$ molar ratio %). When 10%

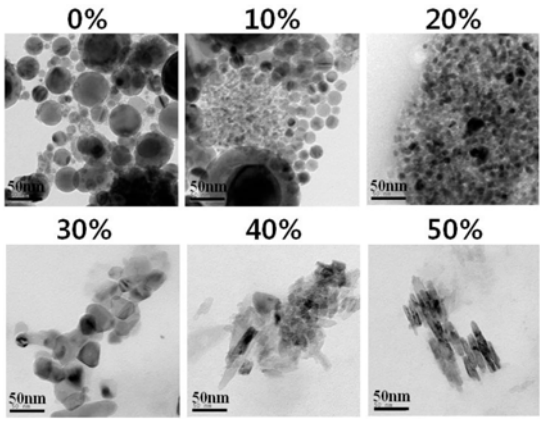

Fig. 7 TEM images of nickel nanoparticles synthesized using electrical discharge in aqueous solution with different initial CTAB doses

CTAB was added, spherical polycrystalline particles were observed like the particles generated without the addition of CTAB. However, the particle size became generally smaller by the addition of 10% CTAB. When 20% CTAB was added, small polycrystalline particles with the diameter of 10 nm were mainly observed. When the added amount of CTAB was 20% or smaller, the particles were aggregated with a very low degree of dispersion. When 30% CTAB was added, larger particles with polygonal (triangular, pentagonal, and hexagonal) shapes were mainly observed. When the amount of CTAB was increased further to 40%, both polygonal and wisker-shaped particles were observed. When 50% CTAB was added, wisker-shaped particles were dominant. The particle size range was measured to be 40~90 nm (0%), 20~60 nm (10%), 10~20 nm (20%), 30~40 nm (30%), 20~70 nm (40%), and 30~50 nm (50%). Particles were spherical for 0~20%.

Fig. 8 compares the TEM images of the nickel particles generated with different length of plasma treatment time. For all the cases, 50% CTAB was added and the initial $NiCl_2$ concentration was 3.3 mM. The effect of the length of plasma-treatment time is clearly shown in this figure. When the plasma treatment was performed for 30 minutes, very small ($\leq$ 10 nm) spherical polycrystalline particles were observed. When the plasma treatment was conducted for 60 minutes or longer, on the other hand, wisker-shaped particles were mainly observed and the particle size and number increased with the length of plasma treatment time. Spherical particles with a size of 5~10 nm were produced at 30 min, whereas after 60 min wisker-shaped particles with sizes of 30~40 nm (60 min), 40~50 nm (90 min), and 40~60 nm (120 min) were obtained.

As was mentioned above, spherical particles are generated when particles are very small, whereas as a particle grows, specific shape may develop to minimize the total surface energy. In order for a surfactant to intervene in the particle growth, it has to combine with the particle surface. The connection between the particle surface and the surfactant takes place selectively for specific surface orientation. It is believed that the generation of sharp columnar crystals shown in Fig. 8 was influenced by this selectivity.

Metal ions can be reduced to zero-valent metal if sufficient amount of electrons are provided. In LPP, large quantity of electrons ware produced, which facilitate the reduction of metal ions to metal

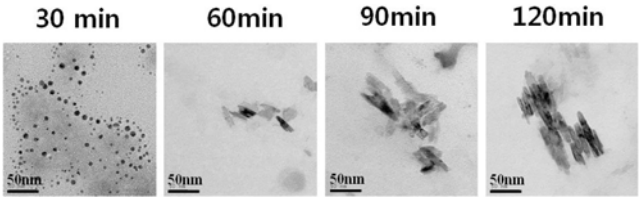

Fig. 8 TEM images of nickel nanoparticles synthesized by different plasma-treated times with CTAB

precipitates in liquid, forming nanoparticle suspension. In this study, the effect of an anionic surfactant (SDS) and a cationic surfactant (CTAB) on the morphology and the size of nickel nanoparticles generated by treating a nickel chloride solution using the LPP method. While the anionic surfactant SDS did not show any significant effect on the particle generation, the cationic surfactant CTAB was shown to exhibit a large influence on the particle generation procedure in various ways. Small spherical nanoparticles were generated with a short plasma treatment time, whereas wisker-shaped nanocrystals were obtained with a long plasma treatment time.

Generally, addition of surfactant influences the nanoparticle generation process through the electrostatic interaction between the nanoparticle surface and the surfactant. Chung and Kang reported that size, morphology, and degree of dispersion of ZnO particles were affected by the surfactant used.[18] Most metal oxides are known to have positive charges on their surface as a result of the formation of hydrophilic colloid due to the hydroxyl or carboxyl groups. Ishikawa et al. argued that the positive ZnO particles were surrounded by anionic surfactant SDS molecules, inhibiting the particle growth, whereas the hydrophobic part of cationic surfactant CTAB is oriented toward ZnO particle surface due to the repulsion between the particle surface and the hydrophilic part of CTAB, promoting continuous particle growth through hydrophobic attraction.[19] In this study, however, the opposite trend was observed; addition of SDS showed no significant effect on the growth of nickel particles, whereas particle growth was suppressed by the addition of CTAB. This result is believed to stem from the opposite charges produced on the surface of metal oxide particles and metal particles.

Metal particles, such as Au, Ag, Fe, and Ni particles, are generally classified as hydrophobic colloid and the charge on their surface, which is usually negative, is determined by the pH of the solution and their concentration. Au and Ag particles exhibit strong repulsive force due to the negative surface charge inhibiting particle aggregation. In order to overcome this phenomenon, efforts have been made to control pH or to lower the zeta potential by combining opposite charges.[20] The surface charge of Fe and Ni particles are determined by the condition of the solution. The negative surface charge induces repulsive force among the particles preventing the particles from coagulating. The zeta potential of the colloid dispersed in a water solution depends on the surfactant added.[21]

A surfactant molecule is composed of a hydrophilic part with electrical charge and a nonpolar hydrophobic part. When an anionic surfactant SDS is added as in this study, SDS molecules are repulsed from the particle surface by Coulomb force due to their negative hydrophilic part. Therefore, addition of SDS imposed little effect on the

growth of nickel particles as was shown in Fig 5. On the other hand, when a cationic surfactant CTAB is used, the positive hydrophilic part of CTAB is oriented toward the surface of negative nickel particle surface, covering the nickel particles effectively and repulsing nickel ions. This effect of CTAB is believed to have led to generation of small nanoparticles shown in Fig 8 (30 min). In our previous study,[22] non-aggregated (therefore, well-dispersed) metal particles could be obtained, regardless of the precursor concentration, by using the same surfactant/precursor ratio.

The chemically active species produced in the LPP were measured using an AvaSpec-3648 Fiber optic spectrometer (Avantes). The excited states of atomic hydrogen, H_α at 656.3 nm and H_β at 486.1 nm, and atomic oxygen, $3p^5P \rightarrow 3s^5S^0$ at 777 nm and $3p^3P \rightarrow 3s^3S^0$ at 844 nm, were detected in the emission spectra, as well as the molecular bands of the hydroxyl radicals OH (at 309 nm). Because not only H radicals that cause extraction of metal ions but also OH radicals that can decompose organics are produced under the experimental condition of this study, the decomposition of surfactant may also occur during the plasma process. Therefore, when the plasma treatment time is too long, the effect of surfactant addition can be suppressed by excessive production of OH radicals, resulting in uncontrolled particle growth as is shown in Fig. 8. Therefore, short plasma treatment time with addition of CTAB is recommended to generate small nanoparticles (≤ 10 nm) using the LPP method.

4. Conclusions

The following conclusions were inferred from the results of synthesis of nickel nanoparticles via LPP reduction method with surfactants:

1. When no surfactant was added, both the number and the size of nanoparticles increased with the length of plasma treatment time and with the electrical conductivity of the reaction solution.

2. The generated nickel nanoparticles had polycrystalline structure. The atomic % composition of the particles was shown to be 73.57% Ni, 23.23% Cu, and 3.20 % W.

3. When an anion surfactant SDS was added, spherical nickel nanoparticles with various sizes were generated, but the effect of SDS addition was not clearly observed.

4. When a cationic surfactant CTAB was added upto 20%, smaller spherical nanoparticles were generated than the no surfactant case. When the amount of CTAB added was 30% or larger, large polygonal or wisker-shaped particles were generated.

5. Long reaction time under the addition of CTAB resulted in suppression of the effect of CTAB due to production of excessive OH radicals. To avoid polygonal and wisker-like shape and to produce small spherical nanoparticles (≤ 10 nm), short reaction time is recommended.

ACKNOWLEDGEMENT

This work was supported by the Technology Innovation Program (10050391, Development of carbon-based electrode materials with 2,000 m^2/g grade surface area for energy storage device) funded By the Ministry of Trade, industry & Energy (MI, Korea).

REFERENCES

1. Sun, S. and Zeng, H., "Size-Controlled Synthesis of Magnetite Nanoparticles," Journal of the American Chemical Society, Vol. 124, No. 28, pp. 8204-8205, 2002.

2. Puntes, V. F., Krishnan, K. M., and Alivisatos, A. P., "Colloidal Nanocrystal Shape and Size Control: The Case of Cobalt," Science, Vol. 291, No. 5511, pp. 2115-2117, 2001.

3. Richmonds, C. and Sankaran, R. M., "Plasma-Liquid Electrochemistry: Rapid Synthesis of Colloidal Metal Nanoparticles by Microplasma Reduction of Aqueous Cations," Applied Physics Letters, Vol. 93, No. 13, Paper No. 131501, 2008.

4. Shon, J. H., Song, I. B., Cho, K. S., Park, Y. I., Hong, J. K., et al., "Effect of Particle Size Distribution on Microstructure and Mechanical Properties of Spark-Plasma-Sintered Titanium from CP-Ti Powders," Int. J. Precis. Eng. Manuf., Vol. 15, No. 4, pp. 643-647, 2014.

5. Lee, J., Yoon, Y. J., Eaton, J. K., Goodson, K. E., and Bai, S. J., "Analysis of Oxide (Al_2O_3, CuO, and ZnO) and CNT Nanoparticles Disaggregation Effect on the Thermal Conductivity and the Viscosity of Nanofluids," Int. J. Precis. Eng. Manuf., Vol. 15, No. 4, pp. 703-710, 2014.

6. Chu, W. S., Kim, C. S., Lee, H. T., Choi, J. O., Park, J. I., et al., "Hybrid Manufacturing in Micro/Nano Scale: A Review," Int. J. Precis. Eng. Manuf.-Green Tech., Vol. 1, No. 1, pp. 75-92, 2014.

7. Patel, J. D., O'Carra, R., Jones, J., Woodward, J. G., and Mumper, R .J., "Preparation and Characterization of Nickel Nanoparticles for Binding to His-Tag Proteins and Antigens," Pharmaceutical Research, Vol. 24, No. 2, pp. 343-352, 2007.

8. Wang, A., Yin, H., Lu, H., Xue, J., Ren, M., and Jiang, T., "Effect of Organic Modifiers on the Structure of Nickel Nanoparticles and Catalytic Activity in the Hydrogenation of p-Nitrophenol to p-Aminophenol," Langmuir, Vol. 25, No. 21, pp. 12736-12741, 2009.

9. Wang, A., Yin, H., Ren, M., Lu, H., Xue, J., and Jiang, T., "Preparation of Nickel Nanoparticles with Different Sizes and Structures and Catalytic Activity in the Hydrogenation of p-Nitrophenol," New Journal of Chemistry, Vol. 34, No. 4, pp. 708-713, 2010.

10. Feng, Y., Yin, H., Wang, A., Xie, T., and Jiang, T., "Selective Hydrogenation of Maleic Anhydride to Succinic Anhydride Catalyzed by Metallic Nickel Catalysts," Applied Catalysis A: General, Vols. 425-426, pp. 205-212, 2012.

11. Knecht, M. R., Garcia-Martinez, J. C., and Crooks, R. M., "Synthesis, Characterization, and Magnetic Properties of Dendrimer-Encapsulated Nickel Nanoparticles Containing< 150 Atoms," Chemistry of Materials, Vol. 18, No. 21, pp. 5039-5044, 2006.

12. Bakovets, V. V., Mitkin, V. N., and Gelfond, N. V., "Mechanism of Ni Film CVD with A Ni(Ktfaa)2 Precursor on a Silicon Substrate," Chemical Vapor Deposition, Vol. 11, No. 89, pp. 368-374, 2005.

13. He, Y., Li, X., and Swihart, M. T., "Laser-Driven Aerosol Synthesis of Nickel Nanoparticles," Chemistry of Materials, Vol. 17, No. 5, pp. 1017-1026, 2005.

14. Liu, Z. P., Li, S., Yang, Y., Peng, S., Hu, Z. K., and Qian, Y. T., "Complex-Surfactant-Assisted Hydrothermal Route to Ferromagnetic Nickel Nanobelts," Advanced Materials, Vol. 15, No. 22, pp. 1946-1948, 2003.

15. Chen, D. H. and Wu, S. H., "Synthesis of Nickel Nanoparticles in Water-in-Oil Microemulsions," Chemistry of Materials, Vol. 12, No. 5, pp. 1354-1360, 2000.

16. Lange, H., Sioda, M., Huczko, A., Zhu, Y., Kroto, H., and Walton, D., "Nanocarbon Production by Arc Discharge in Water," Carbon, Vol. 41, No. 8, pp. 1617-1623, 2003.

17. Saito, N., Hieda, J., and Takai, O., "Synthesis Process of Gold Nanoparticles in Solution Plasma," Thin Solid Films, Vol. 518, No. 3, pp. 912-917, 2009.

18. Chung, Y. K. and Kang, W. K., "Preparation of ZnO Nanoparticles by Laser Ablation of Dispersed ZnO Powder in Solution," Journal of the Korean Chemical Society, Vol. 50, No. 6, pp. 440-446, 2006.

19. Ishikawa, Y., Shimizu, Y., Sasaki, T., and Koshizaki, N., "Preparation of Zinc Oxide Nanorods using Pulsed Laser Ablation in Water Media at High Temperature," Journal of Colloid and Interface Science, Vol. 300, No. 2, pp. 612-615, 2006.

20. Shipway, A. N., Lahav, M., Gabai, R., and Willner, I., "Investigations into the Electrostatically Induced Aggregation of Au Nanoparticles," Langmuir, Vol. 16, No. 23, pp. 8789-8795, 2000.

21. Lu, X., Liu, Q., Huo, G., Liang, G., Sun, Q., and Song, X., "CTAB-Mediated Synthesis of Iron-Nickel Alloy Nanochains and their Magnetic Properties," Colloids and Surfaces A: Physicochemical and Engineering Aspects, Vol. 407, No. pp. 23-28, 2012.

22. Lee, H., Park, S. H., Jung, S. C., Yun, J. J., Kim, S. J., and Kim, D. H., "Preparation of Nonaggregated Silver Nanoparticles by the Liquid Phase Plasma Reduction Method," Journal of Materials Research, Vol. 28, No. 8, pp. 1105-1110, 2013.